

ATOMIC FORCE MICROSCOPE CANTILEVER WITH REDUCED SECOND HARMONIC
FREQUENCY DURING TIP-SURFACE CONTACT

BY

JONATHAN R. FELTS

THESIS

Submitted in partial fulfillment of the requirements
for the degree of Master of Science in Mechanical Engineering
in the Graduate College of the
University of Illinois at Urbana-Champaign, 2009

Urbana, Illinois

Adviser:

Associate Professor William Paul King

ABSTRACT

We describe an atomic force microscope cantilever design for which the second flexural mode frequency can be tailored relative to the first mode frequency, for operation in contact with a substrate. A freely-resonating paddle internal to the cantilever reduces the stiffness of the second flexural mode relative to the first while nearly maintaining the mass of the original cantilever. This strategy allows the ratio of the first two resonant modes f_2/f_1 to be controlled over the range 1.6 – 4.5. The ability to vary f_2/f_1 could improve a variety of dynamic contact-mode measurements.

TABLE OF CONTENTS

CHAPTER 1: INTRODUCTION	1
CHAPTER 2: DESIGN.....	4
CHAPTER 3: EXPERIMENT AND DISCUSSION.....	12
APPENDIX.....	22
REFERENCES	26

CHAPTER 1

INTRODUCTION

The tip of an atomic force microscope (AFM) can measure nanometer-scale surface features and materials properties.¹ Many AFM techniques have been proposed the use dynamic interaction of an AFM tip with a surface; the most widely used are those techniques that measure intermittent contact between an oscillating cantilever tip and a surface.² Tapping mode is advantageous because it is gentle on the surface, making it ideal for biological imaging, as well as providing mechanical property information of surfaces through the phase difference of the probe with its actuator. While this technique has been widely used to measure the properties of materials, there are some properties that cannot be well measured if the tip is not in constant contact with the surface. For this reason, other dynamic approaches employ a tip in constant contact with a moving surface, in which mechanical energy is transferred from the surface, through the cantilever tip, and vibrates the cantilever.³

This type of dynamic contact measurement is used in piezoresponse force microscopy (PFM)⁴, scanning joule expansion microscopy (SJEM)⁵, and for measuring adhesion, contact stiffness, and chemical interactions.^{6,7} These methods make use of a lock-in amplifier to measure the amplitude of the cantilever subjected to a sinusoidal input. For the case of PFM, different polar orientations of the grains result in different expansions of those grains, which allows the cantilever to distinguish between differing orientations. The concept is similar in SJEM, but now the expansion is due to thermal expansion of the materials as they are periodically heated by electrical power dissipation. Although the input for most applications is sinusoidal, it need not necessarily be so. One application, known as Photothermal Induced Resonance (PTIR), involves sending a nano-scale IR pulse to the sample and mapping the

frequency spectra for each material on the sample with sub 100 nm resolution.⁸ Although the nature of the forces imparted to a probe from the substrate vary widely, a limited amount of effort has been placed on tailoring AFM probes to specific dynamic contact mode applications in the commercial world.

Some efforts have been made to research novel probe designs to improve the response of certain techniques, and most of the attempts have focused on the importance of the mechanical resonance spectra of the probe in measuring signals. While most dynamic AFM measurements are made at the first resonant mode, f_1 , higher mode operation can improve contrast and resolution for many measurements.⁹ The relationship between f_1 and cantilever spring constant k , as well as the ratios f_2/f_1 and f_3/f_1 are well known for rectangular cantilevers. Other cantilever shapes provide different relationships between these cantilever characteristics. A number of strategies have been suggested to tune higher mode frequencies through the selective removal of mass along the length of the cantilever, ranging from simple rectangular notches to intricate geometrical cutouts.^{10,11,12,13,14,15} Other strategies add mass to specific locations of the cantilever^{16,17} or vary the cantilever thickness along its length,¹⁸ although these designs are mostly theoretical as they are hard to batch manufacture.

These geometrical alterations enhance probe response a number of AFM applications. Rectangular cutouts have increased sensitivity to material boundaries in Kelvin probe force microscopy (KPFM)¹³. Square notches have been designed to amplify the response of elastic modulus measurements to determine local material properties.¹⁴ These probes also detected features unresolved in fundamental mode operation. Secondary resonating structures loosely coupled to the contact mode probe improve the amplitude response in detecting piezo orientation in PFM by amplifying the probe input¹⁰.

While not all of the modified probes focus on the effects of tuning the mode frequencies, tuning modes can improve AFM imaging in some cases. Tuning higher mode frequencies lower allows higher harmonics to pass through many electronic controllers that do not have the bandwidth to pass higher frequency information. Adjusting higher mode frequencies to harmonic multiples of the fundamental also provides an additional amplification¹⁴. Mode frequency tuning can additionally be useful for tuning the cantilever response to the input signal to the substrate in dynamic contact mode applications. This paper reports an AFM cantilever design for contact mode operation where the ratio of second resonance frequency to first resonance frequency (f_2/f_1) is controllable over the range 1.61 – 4.56, with 3.25 being the ratio of a regular cantilever beam in contact.

CHAPTER 2

DESIGN

For a cantilever operating in intermittent contact with a surface, the frequency of a specific vibration mode can be reduced by removing material from the highest flexural stress locations of that mode.¹⁴ For a cantilever in contact with a surface, the locations of highest flexural stress are in different locations than a freely resonating cantilever. Some mode tuning can be achieved by cutting notches of differing sizes at certain locations along the base of the cantilever beam, but initial results showed that the amount of tuning due to these notches was very minimal (see Figures A.1-A.3). To decrease the f_2/f_1 ratio, mass must be removed from the two max stress locations of the second mode shape, while retaining as much mass as possible at high stress locations in the first mode shape.

Figure 1a shows the proposed AFM cantilever, which has a paddle in the middle of the cantilever that can vibrate freely. The paddle ends are located in the region of maximum stress of the second resonant mode. This strategy provides a larger tuning range over edge cutouts¹⁴ since edge cutouts reduce the mass and do not greatly influence the resonance frequency for contact mode operation. This is due to the fact that the frequency of a mode is roughly proportional to the stiffness and inversely proportional to the mass. This resulted in the removal of stiffness for a mode to be counteracted by the removal of mass from the notches. Thus, to effectively modify the frequency of a mode shape, a way must be found to reduce the stress of that mode without significantly altering the mass of the cantilever. The present design reduces stress at the locations of maximum stress while mostly preserving the cantilever mass.

Figure 1b shows a fabricated cantilever, which was fabricated using an FEI Strata DB235 focused ion beam (FIB) to etch the patterns in a commercial silicon cantilever. The ion emission current was maintained at 2.2 μA with a lens voltage of 30 kV. The emission current was reduced using a 7000 pA aperture to make the milling spot size 150 nm. This aperture choice was chosen based on the feature sizes of the milled areas and time. The etching pattern was constructed from a set of rectangles totaling 836 μm^2 , and the time to etch through 2 μm thick took approximately 1.5 hours. The features were etched with a 1 μs dwell time and a beam overlap of 50%. The cantilever has a length of 350 μm , a width of 35 μm , and a thickness of 2 μm , with a nominal stiffness of 0.3 N/m before modification. The internal paddle has a length of 180 μm and a width of 27 μm , with the axis of rotation at the center of the paddle, located 197 μm from the base of the cantilever beam.

A finite element model simulated the modified cantilever deflection and resonance characteristics to predict cantilever mechanical behavior. The three-dimensional model had an element size sufficiently small so that further decreases in element size resulted in negligible solution changes (see Figure A.4). The boundary conditions of the cantilever fixed the displacement at the base and simply supported the point of the tip to simulate the cantilever in contact with a substrate. A block Lanczos modal analysis produced the mode shapes.

Figure 2 shows the cantilever flexural shape of the first 4 resonant modes. The shapes of the modes provide insight into the high stress locations of the modified cantilever, as well as information about the slope of the cantilever response along the length of the beam, which is the dominant signal for the AFM laser detection.¹⁹ The first mode shape exhibits a half sine standing wave pattern with a maximum at the location of the paddle's axis of rotation. Because the slope at this maximum is always zero, the slope along the entire length of the paddle is

always zero. The second mode shape resembles a full sine standing wave pattern with a maximum slope at the paddle axis of rotation. Thus, the entire length of the paddle similarly contains this maximum slope along the entire length of the beam. The third mode shape is similar to the first, but now the paddle and the cantilever are oscillating out of phase, causing the paddle to flap at each end. The fourth mode shape is similar to the second, with the key difference again being the out of phase motion between the paddle and cantilever.

The mode frequencies were simulated across a range of paddle lengths and widths to better understand the dynamics of the device and to predict the values of the mode frequencies. Figure 3 shows the 1st and 2nd mode frequency response of an internal paddle cantilever 350 μm in length, 35 μm wide, and 2 μm thick as a function of internal paddle length and width. Figure 3a shows the 1st mode frequency, and Figure 3b shows the 2nd mode frequency both as a function of paddle width and length. Figure 3c shows the ratio of the second mode shape to the first. When the paddle width and length are both small, the f_2/f_1 ratio remains close to that of a normal cantilever, which is 3.25. If the paddle width is small and the length is increased, there is a decrease in the second mode frequency as the notches begin to relieve stress in the points of maximum stress in the second mode, while the first mode frequency remains roughly constant. When the paddle is short and wide, most of the stress is relieved in the maximum stress point of the first mode shape, resulting in a spike of f_2/f_1 with a predicted value of 4.5. The ratio is at a minimum when both the length and the width of the paddle are maximized at a value of 1.6. Varying the paddle center of mass and axis of rotation revealed that the ratio was optimized and the response behaved well when the center of mass was on the axis of rotation and when the axis of rotation coincided with the location of maximum slope of the cantilever's second contact mode. Overall, the predictions show that the ratio f_2/f_1 could be tailored over the range 1.6-4.5.

Figure 4 shows the 3rd and 4th mode frequency response of an internal paddle cantilever 350 μm in length, 35 μm wide, and 2 μm thick as a function of internal paddle length and width. Figure 4a shows the frequency dependence on paddle width and length for the 3rd mode, and figure 4b shows the ratio of the 3rd mode to the 1st. Similarly, figure 4c shows the frequency dependence on paddle width and length for the 4th mode, and figure 4d shows the ratio of the 4th mode to the 1st. The cutouts reduce the ratios of both the 3rd and 4th modes in a similar fashion to the second, followed by increases in the ratio for long widths and lengths due to the inclusion of more maximum slope points along the cutouts.

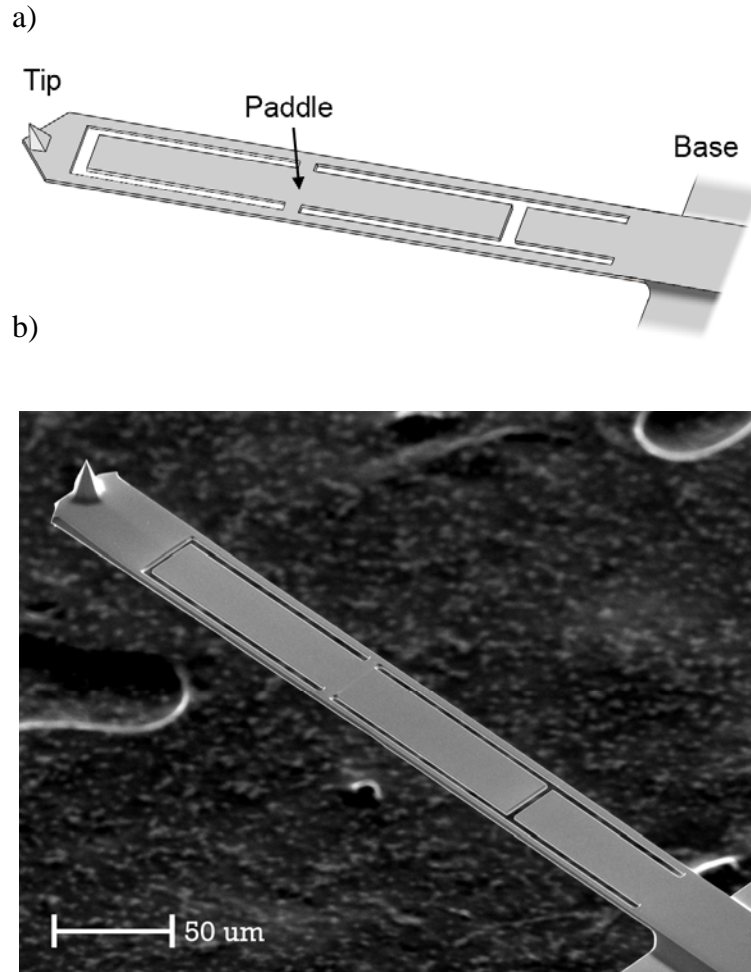


Figure 1: a) Schematic of the cantilever having an internal paddle. The paddle design reduces the high stress locations of the 2nd mode shape while retaining as much original mass as possible. b) Scanning electron microscope image of the modified cantilever fabricated using focused ion beam etching.



Figure 2: First four mode shapes for the internal torsion paddle cantilever fixed at the base and simply supported at the probe tip. The shape of the mode shows where high stress locations are, as well as providing insight into how the laser deflection system of the AFM will detect the probe response along the probe length.

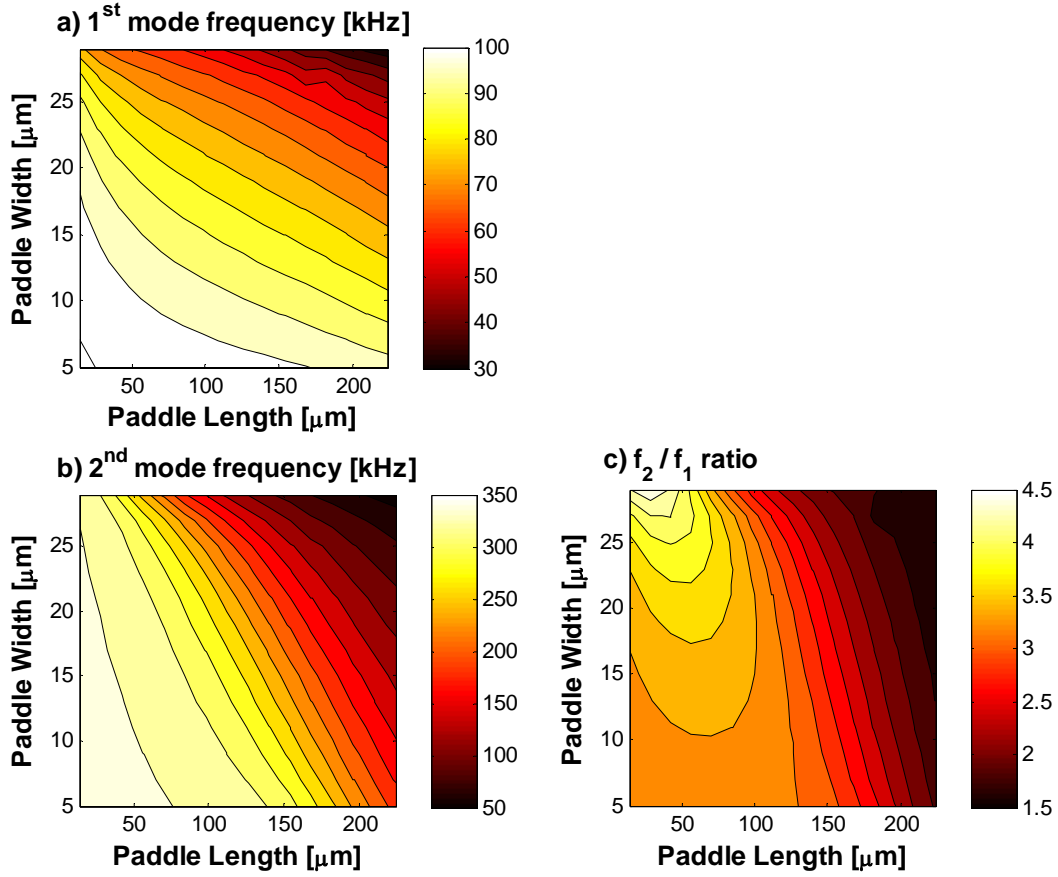


Figure 3: 1st and 2nd finite element mode shape frequencies for an internal paddle cantilever 350 μm in length, 35 μm wide, and 2 μm thick as a function of internal paddle length and width. a) The first mode shape frequency as a function of paddle width and length. b) The second mode shape frequency as a function of paddle width and length. c) The ratio of the second mode frequency to the first.

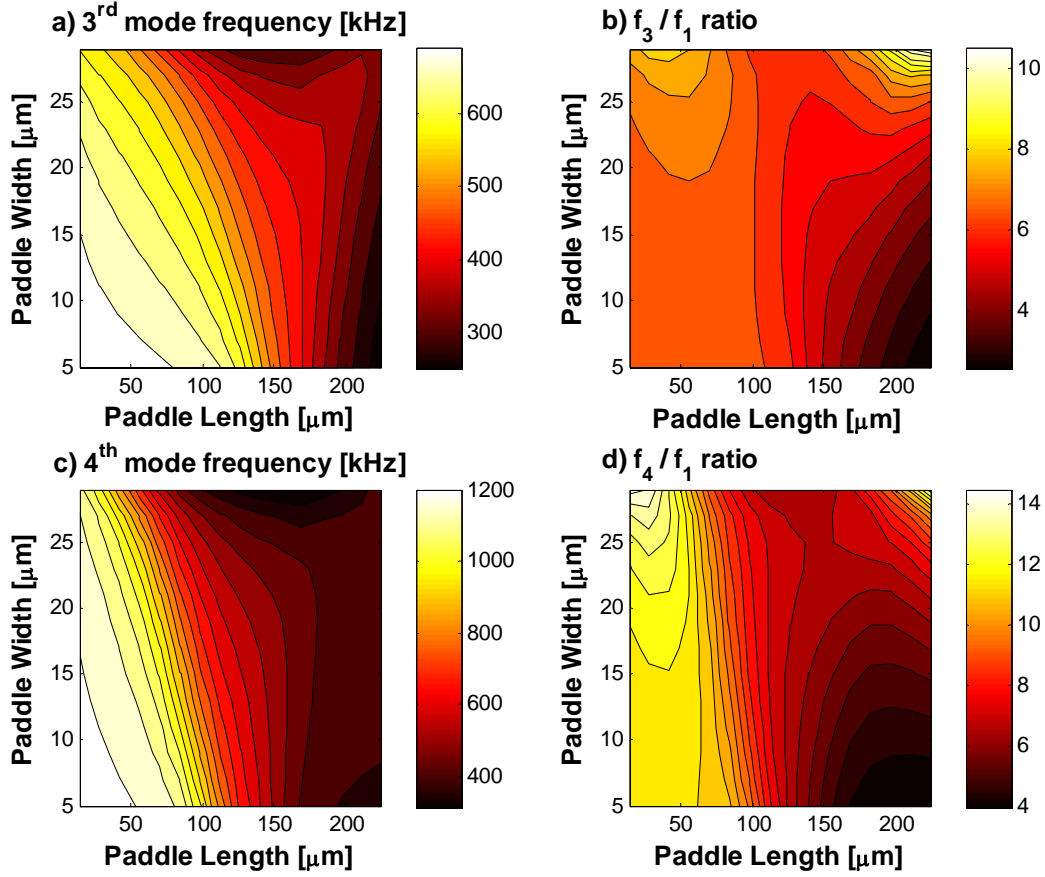


Figure 4: 3rd and 4th finite element mode shape frequencies for a cantilever 350 μm in length, 35 μm wide, and 2 μm thick as a function of internal paddle length and width. a) The third mode shape frequency as a function of paddle width and length. b) The ratio of the third mode frequency to the first. c) The fourth mode shape frequency as a function of paddle width and length. d) The ratio of the fourth mode frequency to the first.

CHAPTER 3

EXPERIMENT AND DISCUSSION

Separate experiments were performed on rectangular cantilevers and cantilevers having the internal paddle. Figure 5 shows the experimental setup. We mounted the cantilevers in our MFP-3D AFM system and we measured their resonance characteristics for the tip out of contact with a substrate and for the tip in contact with the substrate. A piezoceramic actuator served as the substrate for the in-contact experiments, which was driven by a noise signal from a function generator. The detection laser measures the deflection of the cantilever which is collected using the photodiode. The AFM controller integrated the laser input to the photodiode over time to produce the resonance spectra shown. The piezoceramic excitation was necessary to achieve a good signal to noise ratio in the response.

We obtained the frequency spectra for an internal paddle cantilever with the deflection detection laser positioned at various points along the cantilever to compare to the model and to determine the optimal detection point. Figure 6 shows the experimental relationship between position of the reflected laser spot on the cantilever and the measured resonant characteristics for the first two modes of an internal paddle cantilever. When the laser was directed at the end of the cantilever, the frequency spectrum showed a more pronounced first mode and a second mode response roughly 5 times smaller. The third mode response was barely detected, and no higher modes were found. When the laser was positioned on the end of the internal paddle, the frequency spectrum did not detect the first mode shape, confirming the simulation results that the paddle slope does not change at the frequency of the first mode. The second mode response was almost an order of magnitude greater than when the laser was positioned on the tip, and two additional modes beyond the third were detected. All subsequent experiments used a laser

position such that the spot size covered both the tip of the beam and the end of the paddle to find a good balance between detecting the first mode and detecting the larger signal of the second mode from the paddle.

Also of interest is the dependence of substrate amplitude and tip force on mode frequency. Figure 7 shows the first and second mode frequency for an internal paddle cantilever in contact with a poly (methyl methacrylate) substrate for a variety of different piezoceramic actuation amplitudes. The response is very ordered at low powers, but higher powers cause the response to become highly non-linear. 0.04, 0.4, 4, and 40 nm correspond to input voltages across the piezo of 0.1, 1, 10, and 100 V, respectively. These relatively small displacements cause such a high non-linearity because it is the maximum amplitude of a noise signal.

The general influence of tip force on the mode frequencies was also inspected for the internal paddle cantilever. Figure 8 shows the frequency response of the first two modes of the internal paddle cantilever on poly (methyl methacrylate) for a variety of tip-sample forces. The first mode frequency occurs at 54.6 kHz for a 13 nN force, 56.8 kHz for a 39 nN force, and 57.9 kHz for a 54 nN force. The second mode frequency is 81.7 kHz for a 13 nN force, 83.2 kHz for a 39 nN force, and 84.2 kHz for a 54 nN force. Based on this data, the frequency shifts on the order of 100 Hz per nN for the first two modes.

After determining the affect of laser position, substrate excitation amplitude, and tip-sample force, we measured the frequency spectra for both an unmodified rectangular cantilever and a cantilever with an internal paddle. Figure 9 compares the first 2 modes of the unmodified cantilever to the first 3 modes of the modified cantilever. The original rectangular cantilever had in-contact mode frequencies $f_1 = 114.9$ kHz and $f_2 = 333.1$ kHz, with $f_2/f_1 = 2.90$ compared to 3.25 from simulation. The modified cantilever had mode frequencies $f_1 = 53.1$ kHz, $f_2 = 86.9$,

and $f_3 = 334.7$ kHz, with $f_2/f_1 = 1.64$. In addition to the greatly reduced ratio between the second and first mode, the modified cantilever showed a much stronger signal than the unmodified cantilever. Table 1 compares the experimental frequencies with values predicted by finite element analysis, showing good agreement.

Table 1 shows the frequency spectrum for one modified probe with a 350 μm , a width 35 μm , and thickness of 2 μm , an internal paddle length of 180 μm and width of 27 μm , with the axis of rotation 197 μm from the base of the cantilever beam. The cantilever stiffness was determined using the thermal method, and the experimental value was compared to the prediction from finite element analysis. This method relies on the equipartition principle from classical thermodynamics to attempt to equate the mechanical fluctuations of cantilever with its thermal energy.²⁰ Other methods to find the stiffness of the cantilever, such as utilizing nano-indentation, proved problematic because the modified cantilever is softer than 1 N/m.²¹ The error in the thermal method is 45% for the normal cantilever and 100% for the modified cantilever. The error comes from the assumptions that the cantilever geometry is rectangular and that a majority of the thermal energy in the cantilever is stored in the fundamental mode. Even with this error, the modified cantilever has a spring constant about one order of magnitude softer than the unmodified cantilever.

We produced additional cantilevers with a range of paddle widths and lengths and obtained their mode frequencies to compare to the finite element model. Table II shows the first two mode frequencies and the ratio between the two for a cantilever with a length of 350 μm , a width of 35 μm , and a thickness of 2 μm . The paddles were of size 75 μm to 235 μm in length and 10 μm to 29 μm in width. Finite element simulations predicted the device mode frequencies by interpolating between data points. The predictions showed that the experimental data agrees

well with the general contour of the models with less than 30% errors for all but two values. Deviations from the model are attributed to poor tolerances on commercial cantilever thicknesses, as well as FIB instrument alignment error. This data demonstrates that the model is valid for a wide range of paddle sizes, allowing for customization of frequency values and ratios.

This technique shows future promise in the many varied forms of contact atomic force microscopy. The proposed AFM probe demonstrates the ability to tune the second mode frequency to the first, while additionally lowering the probe stiffness. The resulting shape of the modes altered the optical measurement of deflection, so the internal paddle had the same slope along its length as its axis of rotation for the first two modes. Focused ion beam etching allowed simple fabrication with commercially available cantilevers, although once the appropriate design is identified such cantilevers could easily be batch fabricated. The fabricated cantilever characteristics compared well with finite element simulations. This technique to tailor f_2/f_1 over a large range is independent of the value of f_1 and thus it could be applied to cantilevers of arbitrary stiffness for many applications of dynamic contact mode AFM.

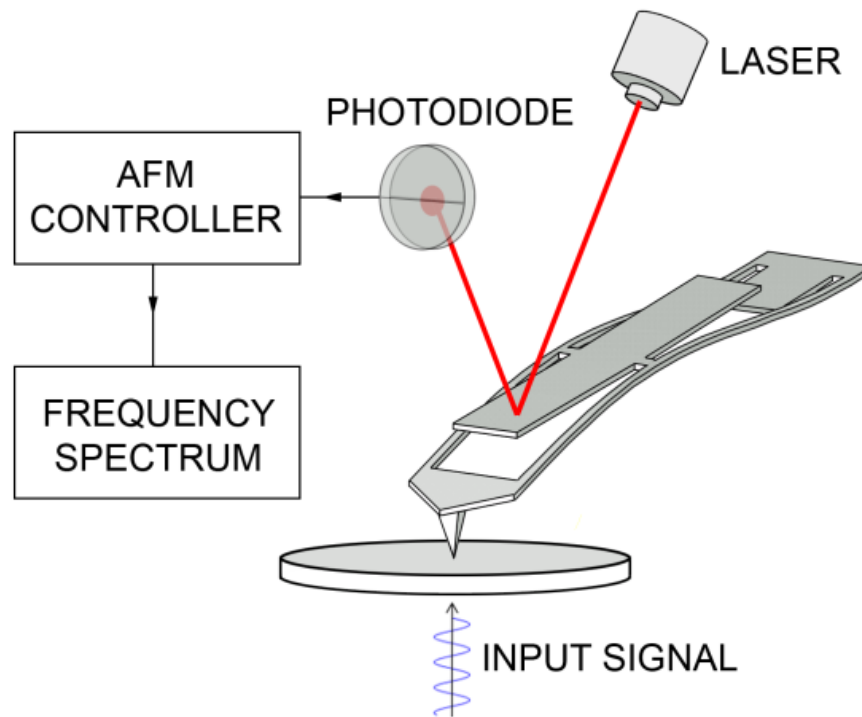


Figure 5: The experimental setup for detecting cantilever frequency response. A piezoceramic actuates the cantilever in contact, and the excitation deflection is captured using a laser and a photodiode. The AFM controller integrated the laser input to the photodiode over time to produce the resonance spectra.

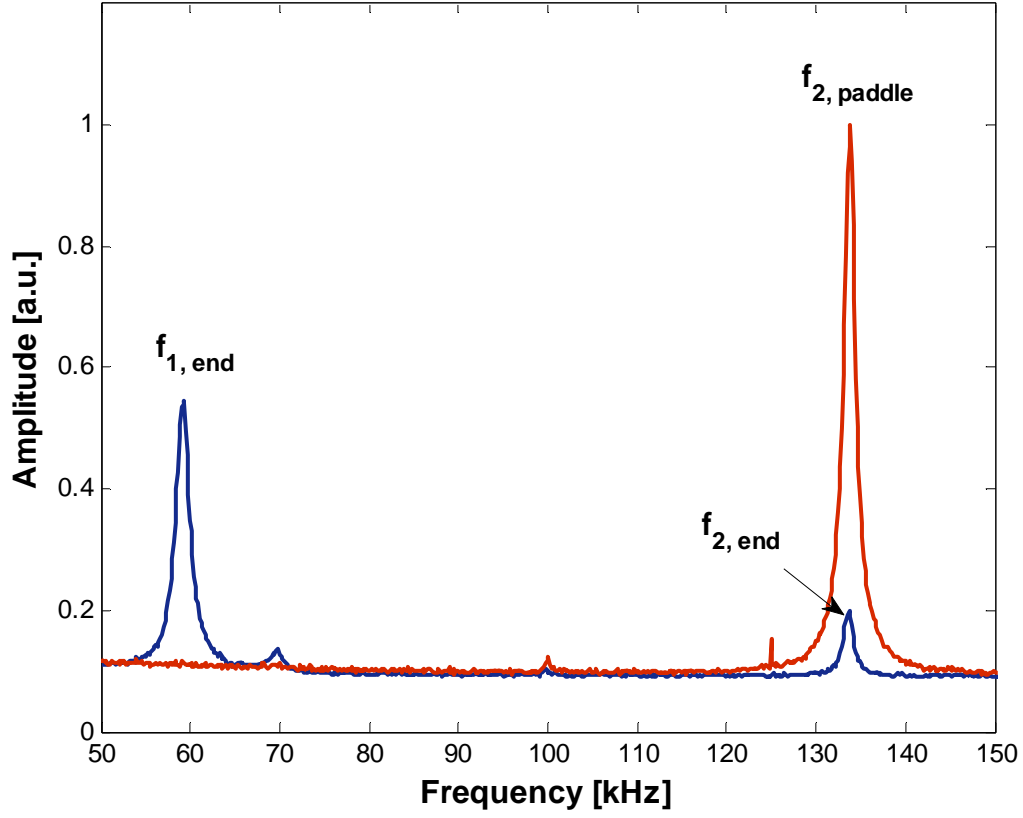


Figure 6: Frequency response of an internal paddle cantilever over the first two modes with the detection laser on the end of the cantilever and on the internal paddle. The first mode is undetected when the laser is on the paddle, which agrees with intuition from the finite element mode shapes. The displacements are typically in the nm range, and are normalized here.

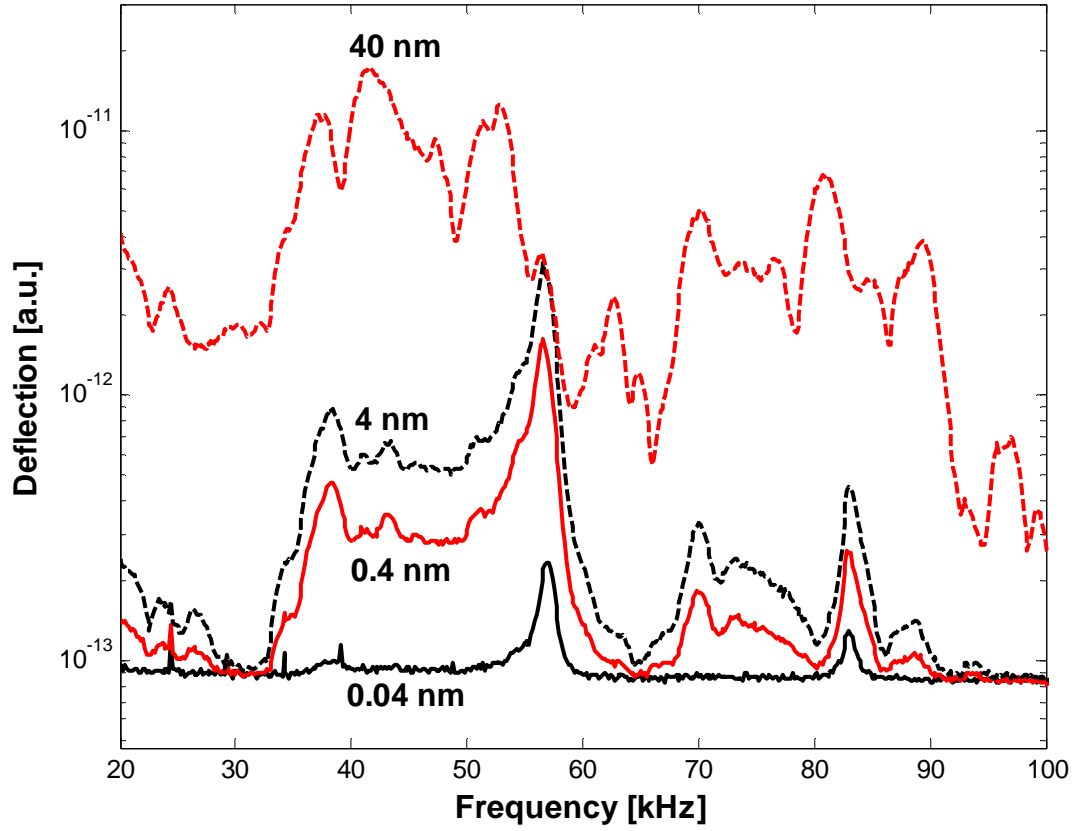


Figure 7: Frequency response of the first two modes for an internal paddle cantilever as a function of input deflection of the piezoceramic actuation stage when the tip is in contact with Poly (Methyl Methacrylate). The response is very ordered at low powers, but higher powers cause the response to become highly non-linear. 0.04, 0.4, 4, and 40 nm correspond to input voltages across the piezo of 0.1, 1, 10, and 100 V, respectively.

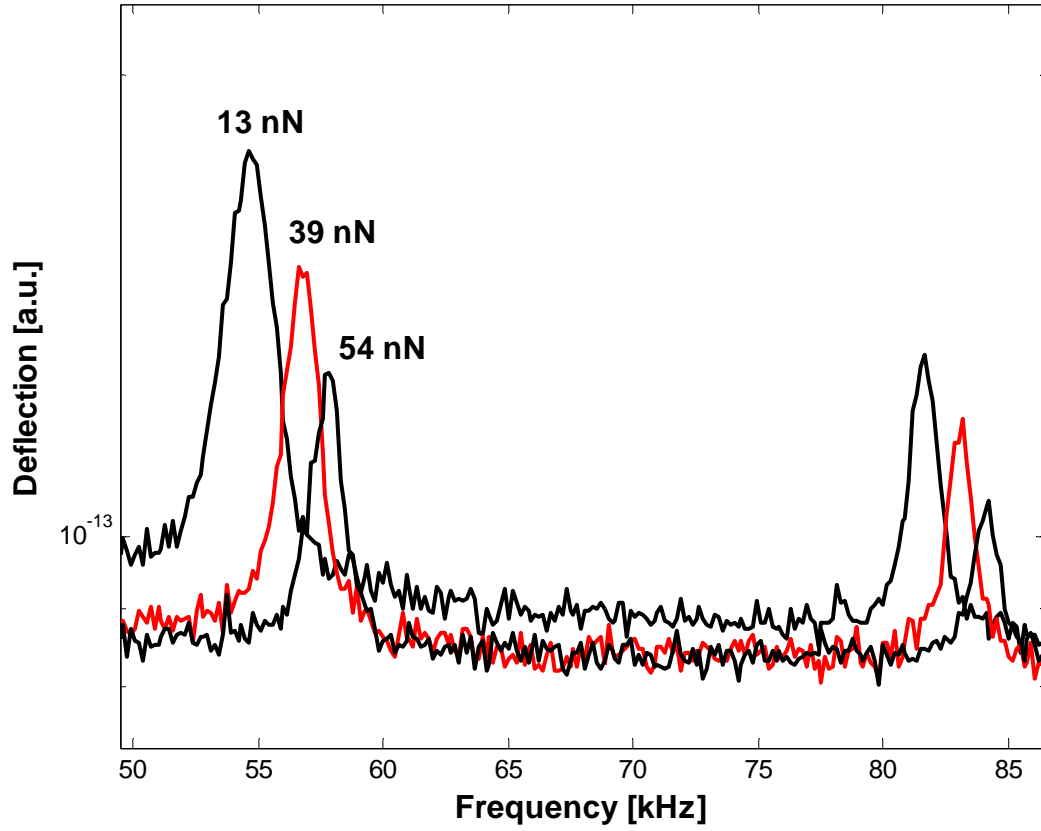


Figure 8: Frequency response as a function of tip force on the substrate for an internal paddle cantilever on Poly (Methyl Methacrylate). The first mode frequency occurs at 54.6 kHz for a 13 nN force, 56.8 kHz for a 39 nN force, and 57.9 kHz for a 54 nN force. The second mode frequency is 81.7 kHz for a 13 nN force, 83.2 kHz for a 39 nN force, and 84.2 kHz for a 54 nN force.

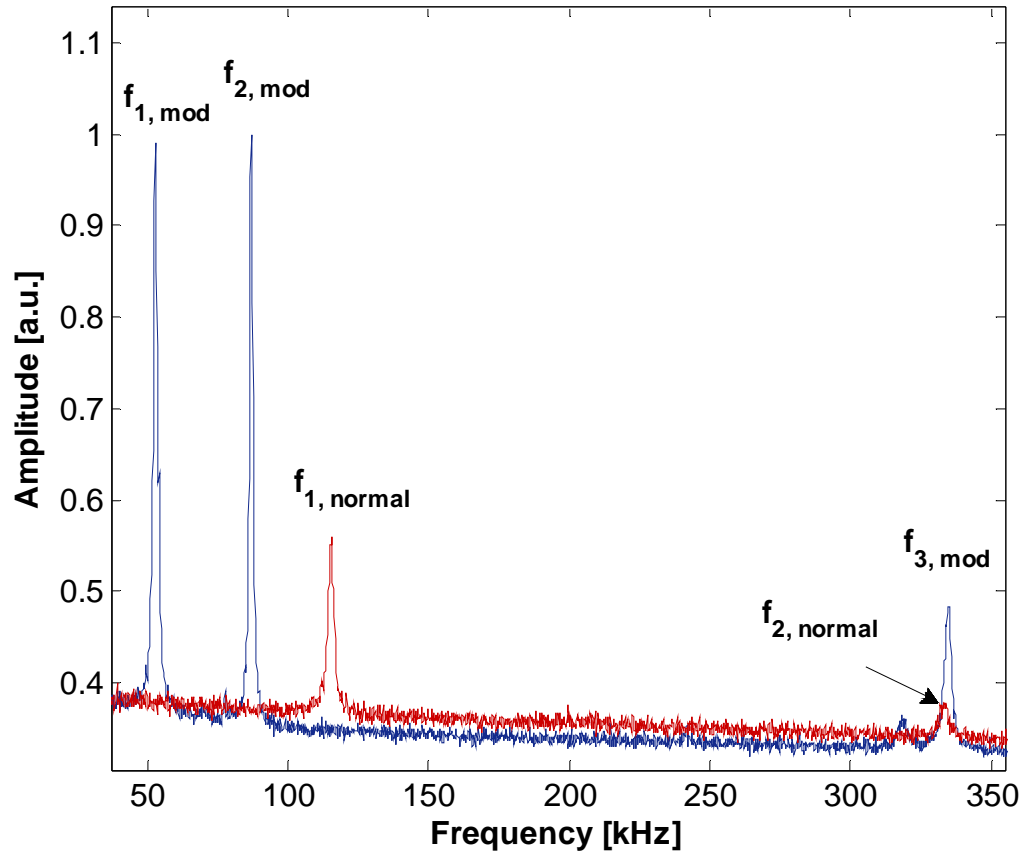


Figure 9: Frequency Spectrum for both a modified (mod) cantilever and the original cantilever. The original cantilever has mode frequencies at 114.9 and 333.1 kHz, with an f_2/f_1 ratio of 2.90. The modified cantilever has mode frequencies at 53.1, 86.9, and 334.7 kHz, with an f_2/f_1 ratio of 1.64 (color online). The displacements are typically in the nm range, and are normalized here.

Table I: Frequency Spectra data for unmodified and modified cantilevers.

		f_1 (kHz)	f_2 (kHz)	f_3 (kHz)	k (N/m)
Modified Probe	Model	50	90	323	0.10
	Experiment	53	87	335	0.05
Original Probe	Model	106	345	717	0.29
	Experiment	115	333	-	0.20

Table II: First two modes across a range of paddle widths and lengths

Paddle Dimensions		Experiment			Prediction		
Paddle Length (μm)	Paddle Width (μm)	f_1 (kHz)	f_2 (kHz)	f_2/f_1	f_1 (kHz)	f_2 (kHz)	f_2/f_1
75	10	108	354	3.28	99	335	3.39
75	29	64	250	3.91	61	204	3.33
155	10	93	231	2.48	93	266	2.85
155	29	56	101	1.80	46	90	1.98
235	10	107	139	1.30	87	161	1.85
235	29	38	51	1.34	32	52	1.62

APPENDIX

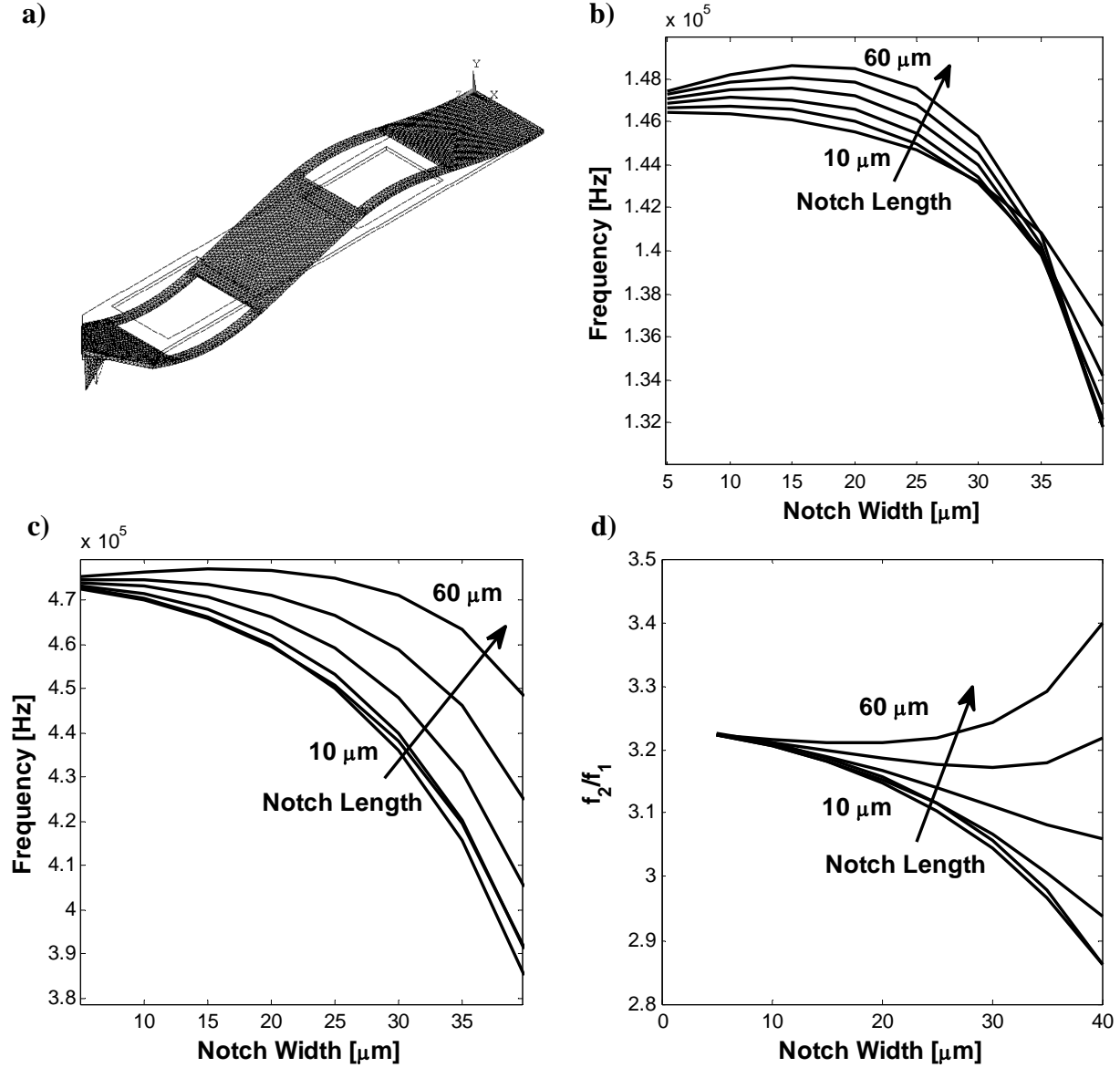


Figure A.1: a) 3D model of an AFM cantilever probe with rectangular cutouts at locations of maximum stress of the second mode with the tip in contact with a substrate. The cantilever is 300 μm long, 50 μm wide, and 2 μm thick. b) Variation of the first mode frequency as a function of both the width and the length of the cutouts. c) Variation of the second mode frequency as a function of cutout width and length. d) The ratio of the second mode frequency to the first for all evaluated rectangular areas.

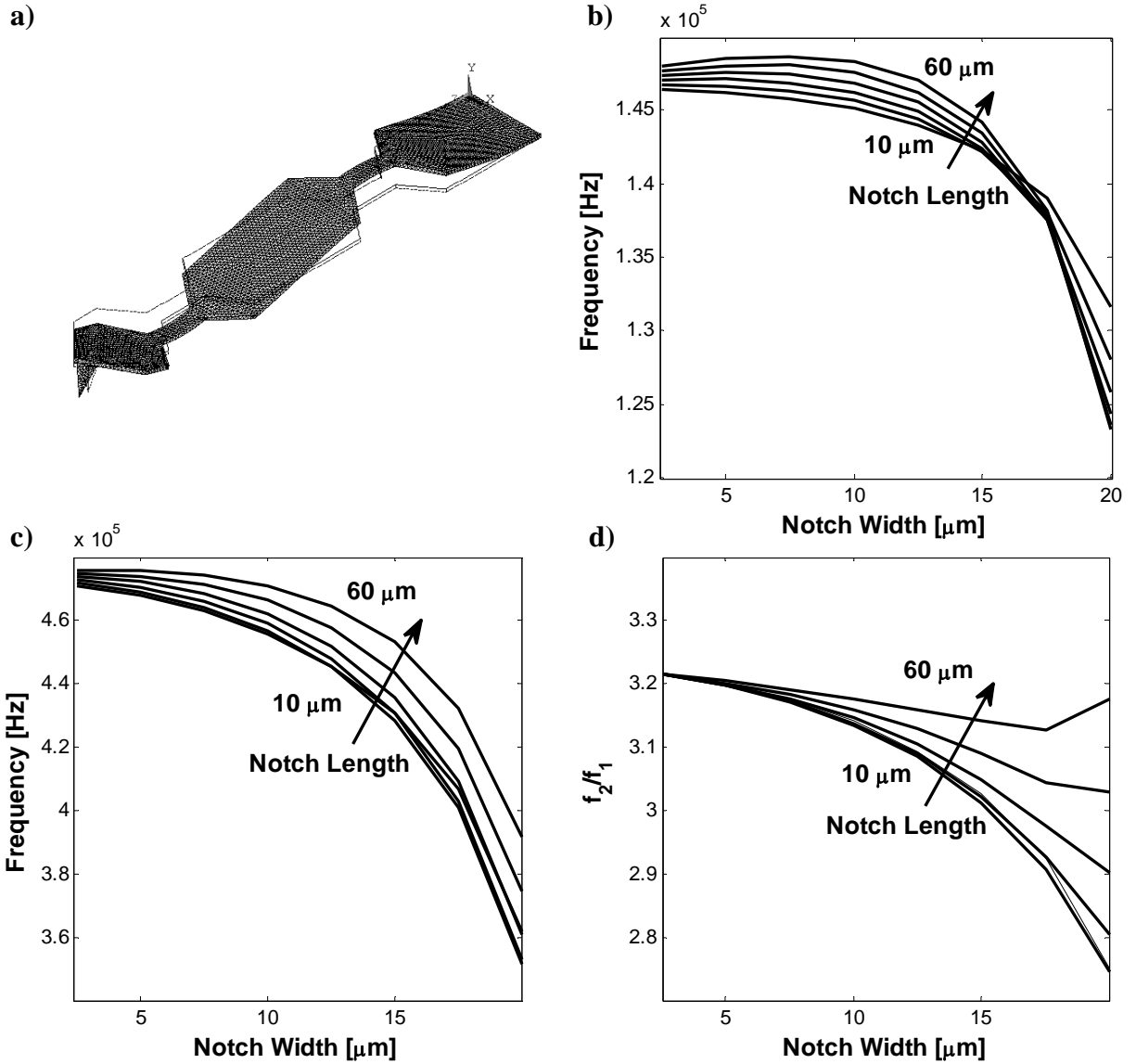


Figure A.2: a) 3D model of an AFM cantilever probe with trapezoidal cutouts at locations of maximum stress of the second mode with the tip in contact with a substrate. The cantilever is 300 μm long, 50 μm wide, and 2 μm thick. b) Variation of the first mode frequency as a function of both the width and the length of the trapezoidal cutouts. c) Variation of the second mode frequency as a function of notch width and length. d) The ratio of the second mode frequency to the first for all evaluated notch areas.

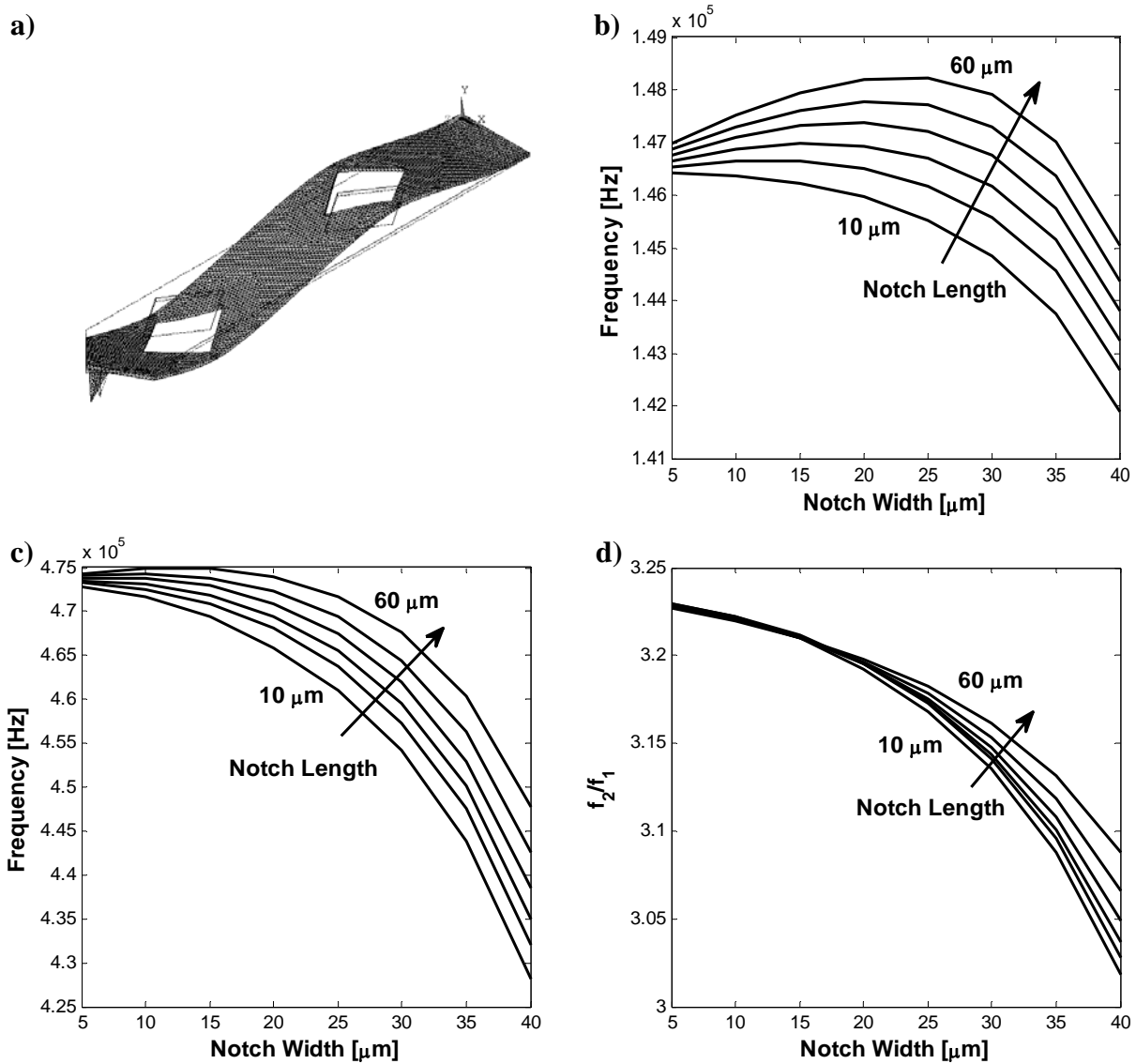


Figure A.3: a) 3D model of an AFM cantilever probe with diamond cutouts at locations of maximum stress of the second mode with the tip in contact with a substrate. The cantilever is 300 μm long, 50 μm wide, and 2 μm thick. b) Variation of the first mode frequency as a function of both the width and the length of the diamond cutouts. c) Variation of the second mode frequency as a function of diamond width and length. d) The ratio of the second mode frequency to the first for all evaluated diamond areas.

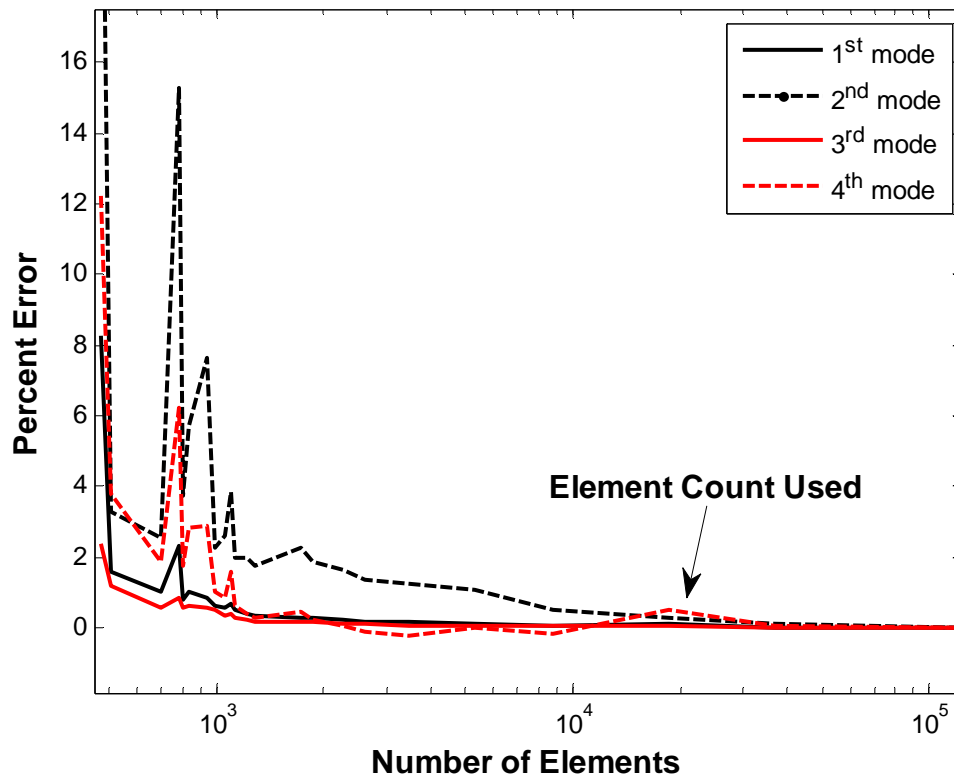


Figure A.4: Convergence test for the finite element analysis for the internal paddle probe. The element count was selected to balance accuracy with time. The maximum error for the element count used is less than 2% as compared to the numerical solution for a model with an order of magnitude more elements.

REFERENCES

- 1 G. Binnig, C. F. Quate, and C. Gerber, "Atomic force microscope," *Phys. Rev. Lett.* **56**
- (9), 930-933 (1986).
- 2 Q. Zhong, D. Inniss, K. Kjoller et al., "Fractured polymer silica fiber surface studied by
- tapping mode atomic-force microscopy," *Surf. Sci.* **290** (1-2), L688-L692 (1993).
- 3 U. Rabe, K. Janser, and W. Arnold, "Vibrations of free and surface-coupled atomic force
- microscope cantilevers: Theory and experiment," *Rev. Sci. Instrum.* **67** (9), 3281-3293
- (1996).
- 4 A. Gruverman, O. Auciello, and H. Tokumoto, "Scanning force microscopy for the study
- of domain structure in ferroelectric thin films," *Journal of Vacuum Science &*
- Technology B: Microelectronics and Nanometer Structures* **14** (2), 602-605 (1996).
- 5 J. Varesi and A. Majumdar, "Scanning Joule expansion microscopy at nanometer scales,"
- Applied Physics Letters* **72** (1), 37-39 (1998).
- 6 C. Daniel Frisbie, F. Rozsnyai, Aleksandr Noy et al., "Functional group imaging by
- chemical force microscopy," *Science* **265** (n5181), p2071(2074) (1994).
- 7 U. Rabe, S. Amelio, E. Kester et al., "Quantitative determination of contact stiffness
- using atomic force acoustic microscopy," *Ultrasonics* **38** (1-8), 430-437 (2000).
- 8 A. Dazzi, R. Prazeres, E. Glotin et al., "Local infrared microspectroscopy with
- subwavelength spatial resolution with an atomic force microscope tip used as a
- photothermal sensor," *Opt. Lett.* **30** (18), 2388-2390 (2005).
- 9 R. W. Stark, T. Drobek, and W. M. Heckl, "Tapping-mode atomic force microscopy and
- phase-imaging in higher eigenmodes," *Applied Physics Letters* **74** (22), 3296-3298
- (1999).
- 10 G. Rinaldi, M. Packirisamy, and I. Stiharu, "Frequency tuning AFM optical levers using a
- slot," *Microsyst. Technol.* **14** (3), 361-369 (2008).
- 11 G. Rinaldi, M. Packirisamy, and I. Stiharu, "Tuning the dynamic behaviour of cantilever
- MEMS based sensors and actuators," *Sens. Rev.* **27** (2), 142-150 (2007).
- 12 B. Zeyen, K. Virwani, B. Pittenger et al., "Preamplifying cantilevers for dynamic atomic
- force microscopy," *Applied Physics Letters* **94** (10), 3 (2009).
- 13 S. Sadewasser, G. Villanueva, and J. A. Plaza, "Special cantilever geometry for the
- access of higher oscillation modes in atomic force microscopy," *Applied Physics Letters*
- 89** (3), 3 (2006).
- 14 O. Sahin, G. Yaralioglu, R. Grow et al., "High-resolution imaging of elastic properties
- using harmonic cantilevers," *Sensors and Actuators A: Physical* **114** (2-3), 183-190
- (2004).
- 15 A. R. Hodges, K. M. Bussmann, and J. H. Hoh, "Improved atomic force microscope
- cantilever performance by ion beam modification," *Rev. Sci. Instrum.* **72** (10), 3880-3883
- (2001).
- 16 A. Maali, T. Cohen-Bouhacina, C. Jai et al., "Reduction of the cantilever hydrodynamic
- damping near a surface by ion-beam milling," *Journal of Applied Physics* **99** (2), 024908-
- 024906 (2006).

- 17 Huiling Li, Yan Chen, and Lanhong Dai, "Concentrated-mass cantilever enhances
multiple harmonics in tapping-mode atomic force microscopy," *Applied Physics Letters*
18 **92** (15), 151903 (2008).
- 18 S. Fernando, M. Austin, and J. Chaffey, "Improved cantilever profiles for sensor
elements," *J. Phys. D-Appl. Phys.* **40** (24), 7652-7655 (2007).
- 19 R. W. Stark, "Optical lever detection in higher eigenmode dynamic atomic force
microscopy," *Rev. Sci. Instrum.* **75** (11), 5053-5055 (2004).
- 20 H. J. Butt and M. Jaschke, "Calculation of thermal noise in atomic force microscopy,"
Nanotechnology **6** (1), 1-7 (1995).
- 21 J. D. Holbery, V. L. Eden, M. Sarikaya et al., "Experimental determination of scanning
probe microscope cantilever spring constants utilizing a nanoindentation apparatus," *Rev.*
Sci. Instrum. **71** (10), 3769-3776 (2000).